Assessing the severity of partial discharges in aerospace applications

Luca Lusuardi, Alberto Rumi, Gabriele Neretti, Paolo Seri and Andrea Cavallini
DEI, University of Bologna
Bologna, Italy
E-mail: luca.lusuardi4@unibo.it

***Abstract*—Current standards base the evaluation of partial discharge (PD) harmfulness on their amplitude and repetition rate. This work shows how, on the contrary, the non conventional environmental conditions introduced by aerospace applications (i.e. low-pressure atmosphere, higher frequency supplies) lead respectively to lower or unchanged PD apparent charges, which are however characterized by different mean energies, hence destructive potential, in a counter intuitive manner.**

***Index Terms*—Frequency, Pressure, More Electric Aircraft, Partial discharges, Insulation, Optical Emission Spectroscopy.**

I. Introduction

Aerospace industry is currently moving towards an aircraft design where more and more electrical systems are replacing non-electrical ones, such as hydraulic, pneumatic or mechanical power transmission. Such choice comes mainly from the simple fact that electrical systems are generally lighter than their alternatives. Weight is one of the main cost-related factors in airlines operation, hence its reduction is usually welcomed by producers and operators.

For the same reason, the additional power that will be required by those added electrical subsystems must be achieved increasing voltage, rather than current (since the latter would require a higher amount of copper). Converters characterized by high power density and fundamental frequencies must be chosen to feed such systems [1], and today power semiconductors supporting this kind of devices are already present on the market. Those are usually characterized by high nominal input voltage, in the order of kV, high ampacity ($100\,\mathrm{A}$), and fast on-times, in the order of tens of ns [2].

Those rather challenging operating conditions are known to be the cause of premature failure of insulating materials. Indeed, the use of impulsive waveforms such as the one being output by a power inverter, with fast transients (i.e. fast rise times), enhances the electrical stress on the insulation system. This is due to (a) an increase of the peak voltage at the machine terminals due to reflections (the surge impedance of the machine is larger than that of the cable) and (b) an increase in the turn-to-turn voltage in proximity of the line terminals due to the inductive/capacitive nature of the stator windings. This will in turn cause an increase in the degradation rate of the insulation, an overall reduction of the reliability of the whole system [3], [4].

If partial discharges are also incepted in defects of the insulation system (e.g. due to the aforementioned electric field magnification effects), additional degradation, hence further life reduction, will be verified.

The severity of the phenomenon is linked to the energy involved in the discharge process, and in particular whether they are able to break the chemical bonds of an insulation, or not. Indeed, IEC 60034-18-41 standard recognize that PD activity is not allowed to incept during the whole life of Type I insulations (typically organic materials) [5].

Standards usually quantify PD activity based on their detected amplitude and repetition rate, without recognizing that the electron energy distribution in a discharge is not necessarily associated to the net amount of charges involved in the process (which is what is quantified by amplitude measurements). The energetic content of a discharge (often referred as "temperature") is, on the other hand, a parameter describing a specific distribution of states among various energy levels of free charge carriers, not their amount.

This distinction is particularly important under the peculiar low-pressure and high frequency conditions an electrical machine operating in an aircraft needs to support. Let us see in the next sections how the application of a novel approach based on PD energy content, rather than their amplitude, will eventually bring to entirely different conclusions regarding the harmfulness of PD activity being detected.

II. Materials and methods

In order to investigate the effect of low-pressure environments, tests were run in a vacuum chamber, specifically designed to feed power to a testing object placed inside of it. Pressures from $1000\,\mathrm{Pa}$ to $100\,000\,\mathrm{Pa}$ were used in this work. A sinusoidal resonant power supply were used to stress the insulations with frequencies ranging from $15\,\mathrm{kHz}$ to $45\,\mathrm{kHz}$.

PD measurements were performed on typical test objects for Type I insulation, that is, twisted pairs (TP) which simulate a turn-to-turn insulation system. Partial discharge inception voltage ($PDIV$) measurements were carried out on 10 samples for each case. This is the lowest voltage at which partial discharges are initiated in the test arrangement when the voltage applied to the test object is gradually increased from a lower value at which no such discharges are observed [5].

The twisted pair were connected inside the vacuum chamber, with a capacitor series on which the charge transferred can be evaluated and a capacitor parallel to obtain the proper

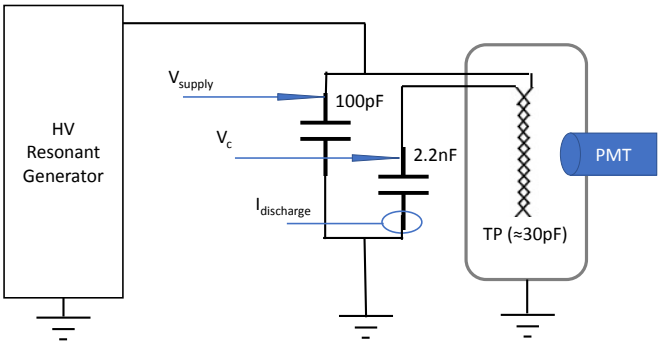

Fig. 1. Circuit diagram for $PDIV$ measurements on twisted pairs by means of PMT.

TABLE I
SUMMARY OF THE TIME STEP LENGTHS FOR EACH PRESSURE CONDITION.

Pressure	Step length
kPa	s
100	60
50	120
10	600
1	600

resonance frequency of the generator. A schematic of the setup is shown in Fig. 1.

In these tests the voltage was raised in step of $25\,\mathrm{V_{pkpk}}$, with a step length dependent on the pressure so to maintain constant the probability of a starting electron [9]. Table I shows the step length values chosen in detail.

Then, a single specimen was used to evaluate both the magnitude and the energetic level of the discharge in each operating condition, imposing a constant peak to peak voltage of $3\,\mathrm{kV}$.

PD were sensed through a Hamamatsu Photo-Multiplier Tube (Head-on PMT H11870). The output signals of the PMT went to a $110\,\mathrm{MHz}$ wide bandwidth Hamamatsu Photon-Counter Unit (C8855-01). The TP and the sensor were kept in total darkness, so that external light did not interfere with the observation of partial discharges. The PMT is virtually immune to electromagnetic noise, making it possible to achieve very high signal-to-noise ratios.

Two Agilent 10076A capacitive-compensated high-voltage probe with a bandwidth of $250\,\mathrm{MHz}$ were used to measure the applied voltage V_{supply} and the voltage drop V_c on the series capacitor, while a Tektronix TCP312 Hall current probe with a bandwidth of $100\,\mathrm{MHz}$ was used to measure the discharge current $I_{discharge}$ of which the maximum was recorded.

The average power freed by the discharges in the time unit was calculated using Lissajous figures, firstly evaluating the total energy by means of (1) and then dividing by the number of periods acquired and multiplying by the frequency.

$$E = \int q(v)dv \tag{1}$$

TABLE II
EXPOSURE TIMES AND NUMBER OF ACQUISITIONS FOR EACH OPERATING CONDITION.

Frequency	Pressure	Exposure time	Number of acquisitions
kHz	kPa	ms	
15	1	50	50
	10	50	50
	50	1000	50
	100	2000	50
25	50	1000	50
45	50	1000	50

The charge $q(V_{supply})$ as function of the supply voltage is obtainable from the voltage drop V_c on the series capacitor.

The energies characterizing the discharges were measured by means of Optical Emission Spectroscopy. Electron, vibrational and rotational temperatures have been evaluated with the following methods [7]. Electron temperature was derived from the ratio between the First Negative System (FNS) band head peak of N2+ and the Second Positive System (SPS) band head peak of N_2. In the present work, the intensities of the FNS band peak of N_2^+ at $391.4\,\mathrm{nm}$ nm and the SPS peak of N_2 at $394.3\,\mathrm{nm}$ were utilised. The vibrational temperature of these excited states of molecular nitrogen was evaluated by using the Boltzmann plot of rovibronic transitions of the SPS radiation from the band head peak intensities of the two spectral windows mentioned above, as described in [6]. The rotational temperature was obtained by comparing the measured spectra of the SPS with the synthetic ones simulated by means of the software SPECAIR® [8]. The measured values of electron and vibrational temperatures derived above were used as input parameters in the SPECAIR® numerical simulations. In the calculations, the translational temperature was assumed to have the same value as the rotational one.

The optical emission of the discharge was measured acquiring the emission through an optic fiber connected to the pressure chamber module. The fiber terminal was connected to Jobin-Yvon HR-460 monochromator (focal ratio f5.3, focal length $460\,\mathrm{nm}$). The entrance slit and the holographic grating were set at $0.15\,\mathrm{mm}$ and 1200 lines/ mm respectively. The output signal of the monochromator was collected by a Stanford Computer Optics 4 Picos ICCD camera (resolution SVGA, pixel size 4.7 x 4.7 $\mu\mathrm{m}^2$) externally triggered by means of the oscilloscope. The collected spectra were calibrated both in wavelength and intensity by means of a low-pressure mercury vapour lamp and a deuterium-halogen light source respectively. Depending on the operating conditions, a certain combination of exposure time and number of acquisitions was chosen. Table II lists the values in detail. The experiments were performed at constant peak to peak voltage of $3\,\mathrm{kV}$.

Fig. 2 shows one of the samples analysed by optical spectroscopy, fed at $3\,\mathrm{kV_{pkpk}}$ and subjected to $10\,000\,\mathrm{Pa}$, on the surface of which there is the presence of PD activity (denoted by the intense violet aura that surrounds it).

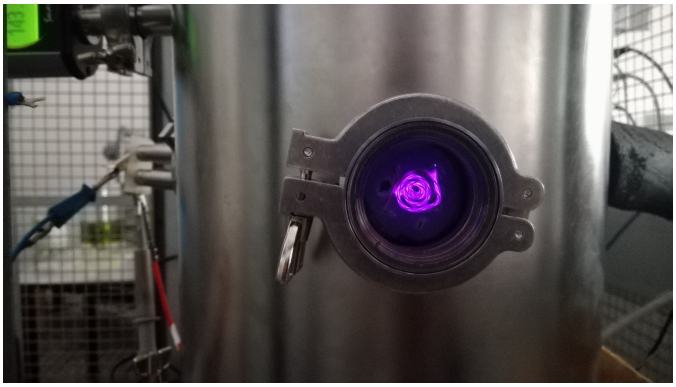

Fig. 2. PD discharge optical emission under 10 kPa.

TABLE III
$PDIV$ AND PHOTON REPETITION RATE DETECTED FOR ALL THE TESTING CONDITIONS.

Pressure kPa	**Frequency** kHz	**PDIV** V_{rms}	**Average emission** s^{-1}
50	15	417.6	1.15e6
	25	427.5	3.17e5
	45	422.6	3.85e5
1	15	340.8	3.35e6
10		294.3	7.51e6
50		417.6	1.15e6
100		558.3	9.90e4

III. Results and Discussion

A. $PDIV$ measurements

Table III summarizes the $PDIV$ levels recorded under different testing conditions. As can be seen, $PDIV$ and repetition rate are mildly influenced by the supply frequency. On the contrary, by decreasing the pressure the $PDIV$ decreases largely, as also reported by other authors [9]–[11].

This must be expected, since with lower pressures a higher mean free path of electrons is expected. This reduces the breakdown field needed to initiate an electronic ionization avalanche, since - on average - free electrons have more and more physical space to accelerate and gather enough kinetic energy from the applied electric field and start a ionization process after a collision with a neutral. A reduced field intensity will then be required to initiate the first electronic avalanche, when pressure is lowered.

However, when the pressure is too low the probability of collision is small, leading to a reversal of the trend of the breakdown field, as in fact is evidenced by the experimental results at 1 kPa, in which the $PDIV$ returns to rise.

The photon emission rate, on the other hand, remains fairly constant for all the cases studied, with the exception of the test carried out at atmospheric pressure. In the latter case, it is likely that the non-rarefied density of the air caused the photons to be absorbed or scattered before reaching the optical sensor, located about 10 cm from the TP area.

Fig. 3 shows, as an example, the progress of a $PDIV$ test.

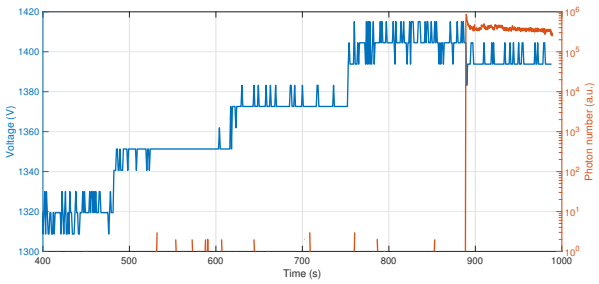

Fig. 3. $PDIV$ measurement performed with PMT at 45 kHz and 50 000 Pa. Blue line is the maximum supplied voltage and red line is the photon emission rate.

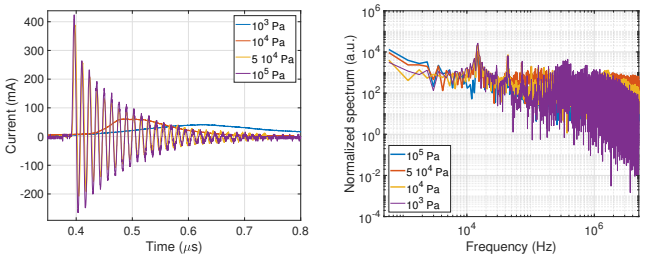

(a) (b)

Fig. 4. PD pulse waveforms (a) and current FFT (b) under different pressures.

B. Impact of pressure

The peak value of the PD current pulse (Fig. 4) is generally reduced for lower pressures. In addition, the time constant that characterizes the impulse also tends to increase significantly as the pressure decreases.

A sudden change in the discharge mechanism from 50 kPa to 10 kPa was observed, as witnessed by the almost flattening of the current pulse. This may be due, given the so low pressure, the $PDIV$ trend analysed above and the voltage and current characteristics just highlighted, to a transition from a partial discharge mechanism to a pseudo-glow one [13].

Table IV summarises the results of the spectroscopic analysis. It is interesting to note that, although the intensity of the detected current peaks tends to decrease with pressure, on the contrary the electrical pulsed power absorbed by the supply and the energy of the emitted photons detected by the spectroscopic analysis increase. This is due to the increase in mean free path electrons can freely travel through, increasing the average kinetic energy electrons will be able to gather in

TABLE IV
PD AMPLITUDE AND ENERGY LEVEL UNDER DIFFERENT PRESSURES.

Press. kPa	**Average power** mW	**Max. PD amp.** mA	**Total charge per cycle** nC	**Electron energy** eV	**PD temp.** K
1	1.25	46.4	690	10.2	400
10	0.90	61.6	390	7.1	400
50	0.43	428	371	6.3	450
100	0.40	536	498	6.8	450

TABLE V
PD AMPLITUDE AND ENERGY LEVEL UNDER DIFFERENT FREQUENCIES.

Freq.	**Average power**	**Max. PD amp.**	**Total charge per cycle**	**Electron energy**	**PD temp.**
kHz	mW	mA	nC	eV	K
15	0.43	428	371	6.3	450
25	1.51	457	280	6.8	450
45	2.21	328	135	7.2	450

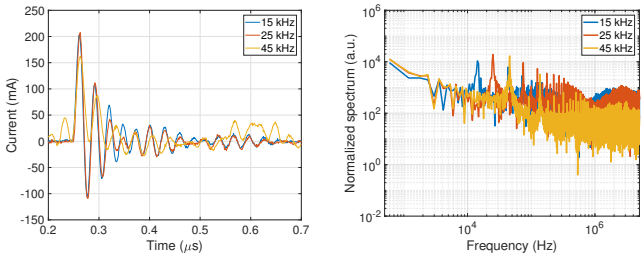

(a) (b)

Fig. 5. PD pulse waveforms (a) and current FFT (b) under different frequencies supplied to the testing specimen.

the discharge process.

This means that destructive mechanisms prevented by the presence of chemical bonds stronger than the typical PD energy at atmospheric pressure are now potentially available, due to the enhanced energetic levels electrons can access in low pressure conditions. Despite a lower PD amplitude, it is possible that low pressure conditions eventually result being much harsher and damaging on an insulation than under atmospheric pressure.

C. Impact of frequency

Table V shows spectroscopy results obtained increasing the frequency fed to twisted pairs. As can be seen, the increase in frequency means that the energy absorbed by the generator is greater, since there are many more discharges in the same interval of time. The electronic energy also increases slightly. This means that at even higher frequencies (think that the new devices in Gallium Nitride can reach even 1 MHz switching frequency [9]) maybe the discharges, in addition to being several orders of magnitude more frequent, are also more energetic, so they are easier to break the polymeric chain bonds.

It should be pointed out that the recorded current signal does not show any significant changes (Fig. 5) although on average the apparent charge measured at each period decreases.

IV. CONCLUSIONS

This paper shows primarily that defining acceptance criteria based on PD amplitude or number, such as the definition of $RPDIV$ given in [5] can result into misleading conclusions regarding the evaluation and design of an insulation for aerospace applications. Indeed, the energy supplied by the power supply, the electron energy and discharge temperature suggest that the most dangerous PD conditions can be found at low pressures and high frequencies.

A definition based on PD energy seems much more effective in predicting the harmfulness of this phenomenon. It is true that there is an added difficulty coming from carrying out this kind of emission spectroscopy measurements, but this is a necessary advancement for a reliable testing of this kind of insulations.

ACKNOWLEDGEMENTS

RAISE project has received funding from the Clean Sky 2 Joint Undertaking under the European Union's Horizon 2020 research and innovation programme under grant agreement No. 785513.

REFERENCES

[1] D. Zhang, J. He and D. Pan, "A Megawatt-Scale Medium-Voltage High Efficiency High Power Density ?SiC+Si? Hybrid Three-Level ANPC Inverter for Aircraft Hybrid-Electric Propulsion Systems," 2018 IEEE Energy Conversion Congress and Exposition (ECCE), pp. 806-813, Portland (OR), 2018.

[2] B. Mouawad, R. Skuriat, J. Li, C. M. Johnson and C. Di Marino, "Development of a highly integrated 10 kV SiC MOSFET power module with a direct jet impingement cooling system," 2018 IEEE 30th International Symposium on Power Semiconductor Devices and ICs (ISPSD), pp. 256-259, Chicago (IL), 2018.

[3] E. Persson, "Transient effects in application of PWM inverters to induction motors," IEEE Transactions on Industrial Applications, vol. 28, pp. 1095-1101, 1992.

[4] A. Cavallini, D. Fabiani and G. C. Montanari, "Power electronics and electrical insulation systems - Part 2: life modelling for insulation design," in IEEE Electrical Insulation Magazine, Vol. 26 , No. 3, pp. 7-15, 2010.

[5] IEC 60034-18-41, "Rotating electrical machines - Part 18-41: Partial discharge free electrical insulation systems (Type I) used in rotating electrical machines fed from voltage converters - Qualification and quality control tests," 2013.

[6] C.A. Borghi, A. Cristofolini, G. Grandi, G. Neretti and P. Seri, "A plasma aerodynamic actuator supplied by a multilevel generator operating with different voltage waveforms," in Plasma Sources Science and Technology, Vol. 24, 2015.

[7] G. Neretti, et al., "Characterization of a dielectric barrier discharge in contact with liquid and producing a plasma activated water," in Plasma Sources Science and Technology, Vol. 26, No.1, 2017.

[8] C. O. Laux, "2008 Optical Diagnostics and Collisional-Radiative Models," Von Karman Institute Course on Hypersonic and Cruise Vehicles, Stanford University.

[9] D. R. Meyer, A. Cavallini, L. Lusuardi, D. Barater, G. Pietrini and A. Soldati, "Influence of impulse voltage repetition frequency on RPDIV in partial vacuum," in IEEE Transactions on Dielectrics and Electrical Insulation, vol. 25, no. 3, pp. 873-882, June 2018.

[10] R. Rui and I. Cotton, "Impact of low pressure aerospace environment on machine winding insulation," 2010 IEEE International Symposium on Electrical Insulation, San Diego, CA, pp. 1-5, 2010.

[11] A. Cavallini and G. C. Montanari, "Effect of supply voltage frequency on testing of insulation system," in IEEE Transactions on Dielectrics and Electrical Insulation, vol. 13, no. 1, pp. 111-121, Feb. 2006.

[12] T. J. . Hammarstrm, T. Bengtsson and S. M. Gubanski, “Partial discharge characteristics in motor insulations under exposure to multi-level inverters,” 2017 IEEE Conference on Electrical Insulation and Dielectric Phenomenon (CEIDP), pp. 307-310, Fort Worth (TX), 2017.

[13] R. Bartnikas and J. P. Novak, “On the character of different forms of partial discharge and their related terminologies,” in IEEE Transactions on Electrical Insulation, vol. 28, no. 6, pp. 956-968, Dec. 1993.